



## INTERACTION EFFECT ON CABLE-CONNECTED ELECTRICAL EQUIPMENT

K.-J. HONG<sup>1</sup>, A. DER KIUREGHIAN<sup>2</sup> and J. L. SACKMAN<sup>3</sup>

### SUMMARY

Dynamic interaction between electrical substation equipment connected by conductor cables is identified as a possible cause of damage to such equipment during earthquakes. The conductor cable is typically made of helically wrapped aluminum strands. Under bending, the strands tend to slide against each other when an imbalanced tension force in the strand exceeds the maximum friction force that can be generated. The result is a reduction in the flexural stiffness of the cable and energy dissipation under cyclic loading. Thus, the bending moment-curvature-tension behavior of the cable is analogous to the behavior of a rod made of an elasto-plastic material. Additionally, under dynamic loading, the cable experiences large displacements and rotations. In this paper, a newly developed finite element model is described, which properly accounts for the material and geometric nonlinearities of the cable. This model is used to investigate the effect of dynamic interaction between pairs of equipment items connected by various cables. It is shown that, on account of the interaction effect, the response of an equipment item in the connected configuration can be strongly amplified relative to its response in the stand-alone configuration. Slackness can be provided in the cable to reduce the interaction effect. However, amplification may occur in heavy cables with large slack due to the cable inertia. The results in this study provide guidance in selecting cable slackness and in assessing the seismic demand on connected equipment items.

### INTRODUCTION

A typical electrical substation consists of a complex set of interconnected equipment items, such as transformers, circuit breakers, surge arresters, capacitor banks, disconnect switches, etc., many of which support fragile elements such as ceramic bushings. These equipment items are usually connected to each other by rigid or flexible conductors. Due to their dissimilar characteristics, significant dynamic interaction between the connected equipment items may occur during seismic disturbances. Post-earthquake field investigations have revealed that this kind of interaction is responsible for some of the observed damage in electrical substations in past earthquakes (Benuska [1], Hall [2], Schiff [3]).

---

<sup>1</sup> Consulting Engineer, Ajit S. Randhava & Assoc., La Mirada, CA, USA.

<sup>2</sup> Taisei Professor of Civil Engineering, University of California, Berkeley, CA, USA, Email: [adk@ce.berkeley.edu](mailto:adk@ce.berkeley.edu)

<sup>3</sup> Professor Emeritus of Engineering Mechanics, University of California, Berkeley, CA, USA.

This paper investigates the effect of interaction in equipment items connected by flexible conductors, commonly known as conductor cables. The conductor cable is typically made of multiple layers of helically wrapped aluminum strands with alternating lay angles, as shown in Figure 1. Under tension, friction forces develop between the strands. As the cable is bent, an imbalanced tension force develops in each strand segment, which tends to slide the strand relative to its neighboring strands. Sliding occurs when the imbalanced tension force exceeds the maximum friction force that can be generated. As a result of this phenomenon, the conductor cable has a nonlinear flexural behavior: Under a constant tension force, the flexural stiffness decreases as the cable curvature increases and more strands slide. Upon reversal of bending, the strands stop sliding and the initial flexural stiffness is regained. Thus, an elasto-plastic behavior in bending under constant tension is observed. For a typical conductor cable, the flexural stiffness varies between two extreme values, which can be different by as much as two orders of magnitude. In the first section in this paper, we briefly describe a micro-scale flexural model of the helically wrapped conductor cable that has been developed in Hong [4] and Hong [5]. The model considers the state of each individual strand in the cable as a function of the cable curvature and average axial strain.

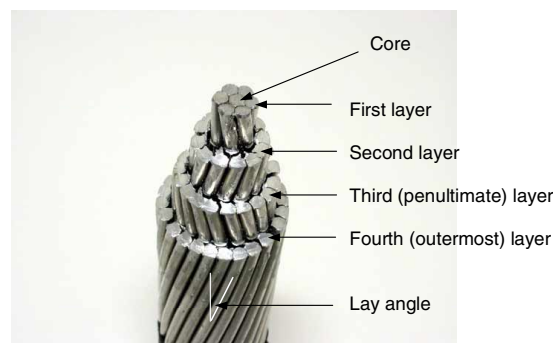


**Figure 1. Typical helically wrapped conductor cable**

Under dynamic load, the conductor cable connecting two equipment items experiences large deformations. Therefore, in order to investigate the effect of interaction between two cable-connected equipment items, one needs to properly model the nonlinear flexural behavior of the cable cross section described above, as well as the nonlinear geometrical effects resulting from the large deformations of the cable. For this purpose, we have fitted a macro-scale flexural model to the micro-scale model of the cable and implemented the element in the finite element code FEAP (Taylor [6]) for large-deformation dynamic analysis. This model is briefly described in the second section below. The finite element model is then used to investigate the effect of interaction between electrical substation equipment with varying characteristics.

In a previous study (Hong [7]), we investigated the effect of interaction between cable-connected equipment items, where the effect of strand slippage was approximately considered by using a reduced flexural stiffness, which remained constant in time and along the cable. The present study aims at refining this analysis by using the elasto-plastic bending model of the cable, which properly accounts for the slippage of strands in the cable. Specifically, the flexural stiffness of the cable is allowed to vary along the cable and in time, depending on the curvature and tension force at each cross section of the cable and the history of loading. The effect of energy dissipation due to slippage of strands is investigated by comparing the response predictions based on the fully-slipped elastic and elasto-plastic models. The results show that, as a result of the dynamic interaction as well as cable inertia, the response of a connected equipment item can be strongly amplified in relation to its stand-alone response, particularly when the conductor cable has small slackness and large mass. These results confirm and extend our earlier findings in Hong [7].

## FLEXURAL BEHAVIOR OF THE CONDUCTOR CABLE

As shown in Figure 1, the conductor cable is made of a core and multiple layers of aluminum strand with alternating lay angles. Table 1 lists the main characteristics of two conductor cables commonly used in the power industry.  $I_{\max}$  in this table refers to the moment of inertia of the cable cross section as a single solid, whereas  $I_{\min}$  refers to the sum of the moments of inertia of the individual strands. As described below, the effective moment of inertia of a conductor cable under dynamic loading varies between these two extreme values. We use these cables in example connected systems later in this paper.

**Table 1. Properties of selected conductor cables**

Property	Valerian	Trillium
Young's modulus, N/m <sup>2</sup>	70×10 <sup>9</sup>	70×10 <sup>9</sup>
number of layers except core	2	6
number of strands	19	127
strand diameter, mm	2.913	3.904
overall conductor diameter, mm	14.57	50.75
cross section area, mm <sup>2</sup>	119	1,423
mass per unit length, kg/m	0.323	3.859
lay angle, degree	12	12
$I_{\max}$ , mm <sup>4</sup>	1,496	227,305
$I_{\min}$ , mm <sup>4</sup>	66	1,417

Consider a differential segment of the cable under axial tension  $T_c$  and bending moment  $M_c$ , and a typical strand in the outermost layer of lay angle  $\alpha$ , as shown in Figure 2. Due to the difference  $dy$  in the vertical distance from the centroidal axis of the cross section to the two ends of the strand, the bending stresses at the two ends of the strand element are slightly different. As a result, the resultant tensile forces acting at the two ends of the strand element are different by the amount  $dt$ . This “imbalanced” tension force tends to slide the strand in the direction of increasing tension. On the other hand, the tensile force in the wrapped strand induces a normal force  $dN$  on the strand element and a resulting friction force  $dF = \mu dN$ , as shown in the right side of Figure 2, where  $\mu$  is the friction coefficient. If  $dF = dt$ , the strand remains in a stick state; if  $dF < dt$ , the strand slides and a redistribution of forces occurs until equilibrium is reached. The situation is similar for strands in the inner layers, except that normal and friction forces act on both inner and outer surfaces of the inner strands.

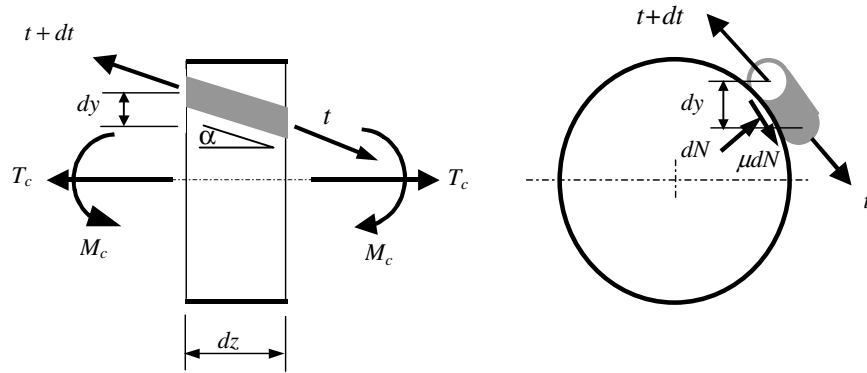


**Figure 2. Forces acting on a differential element of the cable and strand**

In Hong [4] and Hong [5], a detailed model of the helically wrapped cable is developed considering all the stick and slip states of the strands. Account is made of differing lay angles and strand diameters in different layers. A full description of this model is beyond the scope of this paper. Instead, we provide a brief description of the general characteristics of the flexural behavior of the cable as predicted by this model. These predicted characteristics are consistent with experimental observations by, e.g., Raof [8].

Initially, when the cable is in its straight configuration under tension, all the strands are in the stick state and the flexural stiffness of the cable is equal to the elastic modulus of the material times the moment of inertia of the cross section when it is considered as a single solid section. We denote this moment of inertia as  $I_{\max}$ . As the bending moment is applied and increased, strands start to slip as soon as the imbalanced force in a strand exceeds the maximum friction force that can be generated. It is found that slippage first occurs in the outermost layer in the strands located near the centroidal axis (slightly on the compression side of the bending) of the cable, where the differential vertical distance  $dy$  is largest. As the bending moment increases, slippage propagates to other strands in the tangential and radial directions on both sides of the cable. The slippage propagates radially inward because inner layers have larger normal and friction forces than the outer layers and, therefore, tend to slip under larger curvatures. Figure 3 shows the configuration of strands in a partially slipped state of the cable. As the bending moment increases, more strands slip and the effective flexural stiffness of the cross section decreases. For large curvatures, effectively all strands are sliding. In this case the flexural stiffness is slightly greater than the sum of the flexural stiffnesses of the individual strands, denoted  $I_{\min}$  in Table 1, because of the contribution of the frictional forces. We note that the ratio  $I_{\max}/I_{\min}$  can be larger than 100.

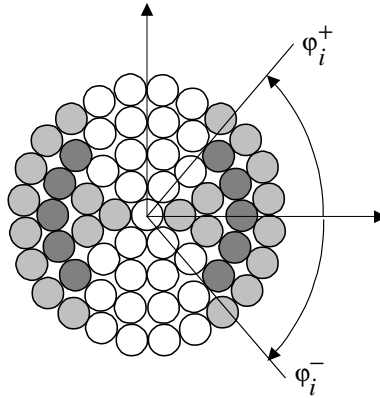


**Figure 3. Strands in a conductor cable in stick (un-shaded) and slip (shaded) states**

Figure 4 shows the bending moment-curvature relations for Valerian and Trillium conductor cables for different average axial strain values of the cable. These are computed by the micro-model in Hong [4] with the friction coefficient  $\mu = 0.3$ . Figure 5 shows plots of the flexural stiffnesses as functions of the cable curvature for constant values of the average cable axial strain. It is seen that the bending behavior of the cable under tension is analogous to that of an elasto-plastic material. The initial stiffness is that of the fully stuck cable, whereas the post-yielding stiffness is that of the fully slipped cable. As mentioned earlier, upon unloading at any point, the flexural stiffness reverts back to the fully stuck value. This is because the direction of impending motion then opposes the imbalanced force.

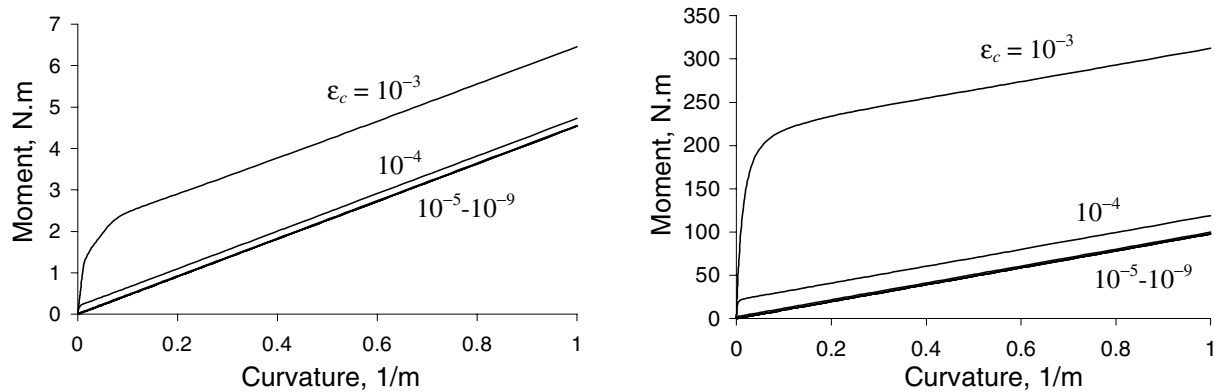


**Figure 4. Bending moment-curvature relations for Valerian (left) and Trillium (right) conductor cables for varying average axial strain in the cable**

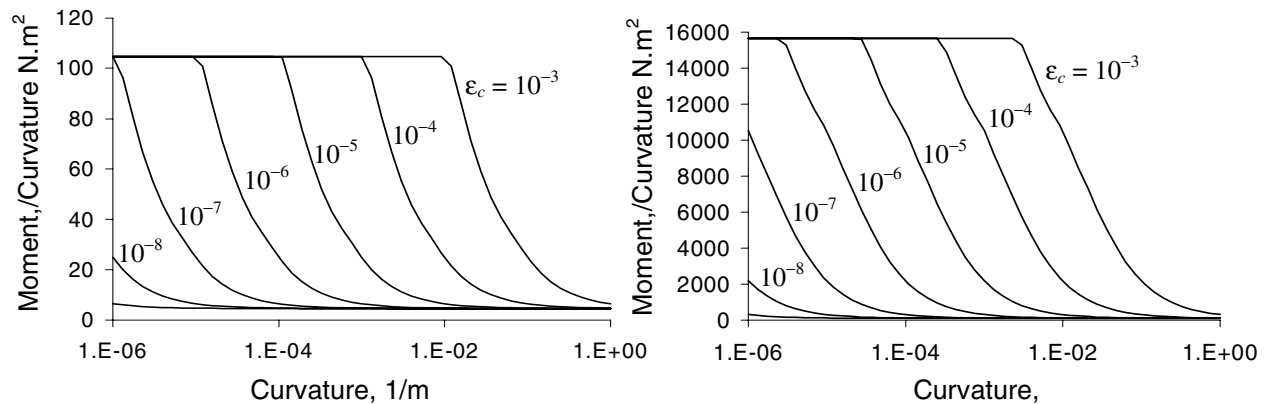


**Figure 5. Flexural stiffness of Valerian (left) and Trillium (right) conductor cables for varying cable curvature and average axial strain**

### FINITE ELEMENT MODEL FOR CABLE DYNAMICS

To construct a finite element model of the cable, consideration should be given not only to the nonlinear bending moment-curvature-tension relation, but also to geometrical nonlinearities arising from large deformations of the cable under dynamic loading. Because of its relatively small flexural stiffness, the cable experiences both large displacements and rotations. To address these nonlinear geometrical effects, it is convenient to utilize the general theory of elastic rods developed by Cosserat [9]. Simo [10] and Simo [11] have developed a finite element formulation based on this theory, but only for elastic rods. To deal with the nonlinear dissipative moment-curvature-tension relation, we model the cable as if it were a solid rod made of an elastic-plastic material, whose hysteretic behavior replicates that of the cable caused by the slippage of strands. The formulation by Simo and Vu-Quoc is extended to develop a finite element model that accounts for both the nonlinear moment-curvature-tension relation and the geometrical nonlinearity of the cable. The extended formulation is implemented in the finite element code FEAP (Taylor [6]), which is used for the analysis reported in this paper. For time-integration, the HHT algorithm by Hilber [12] is used.

In this study, we only consider the case where the motion of the cable is restricted to a fixed vertical plane. The geometrically exact rod theory that models this 2-dimensional problem of the cable and the elastoplastic constitutive law that mimics the nonlinear dissipative behavior of the cable are described in Hong [4]. The interested reader is referred to this publication for details on these developments.

### CABLE-CONNECTED EQUIPMENT SYSTEM

To investigate the effect of dynamic interaction, we consider two equipment items idealized as single-degree-of-freedom (SDOF) oscillators and connected by a conductor cable, as shown in Figure 6. Multi-degree-of-freedom equipment items are idealized as SDOF oscillators by employing an appropriate displacement shape, as described in Der Kiureghian [13]. Thus, each equipment item is characterized by its effective mass  $m_i$ , natural frequency  $\omega_i$ , and damping ratio  $\zeta_i$ ,  $i = 1, 2$ . Given these parameters, the effective stiffness of each equipment is obtained as  $k_i = m_i\omega_i^2$ . Let  $u_1(t)$  and  $u_2(t)$  denote the displacement responses of the two equipment items at their respective attachment points, as shown in Figure 6. The connecting cable is characterized by its compositional properties, i.e., the number of layers, the number of strands, the lay angles, strand and core diameters, the coefficient of friction between strands, the elastic modulus of the material, the weight  $w$  per unit length, and its geometric properties, i.e., the initial arc length  $s_0$ , the initial span  $L_0$ , and the vertical offset  $H$ . The last three parameters are defined in the static equilibrium position of the system. In this position, the cable is stressed under its own weight. Therefore,  $s_0$  is slightly longer than the un-stretched length of the cable, and  $L_0$  is slightly smaller than the distance between the equipment items when they are not connected. The initial chord length is given by  $c_0 = (L_0^2 + H^2)^{1/2}$ . The connected system is subjected to the horizontal base motion  $x_g(t)$  in the plane of the cable.

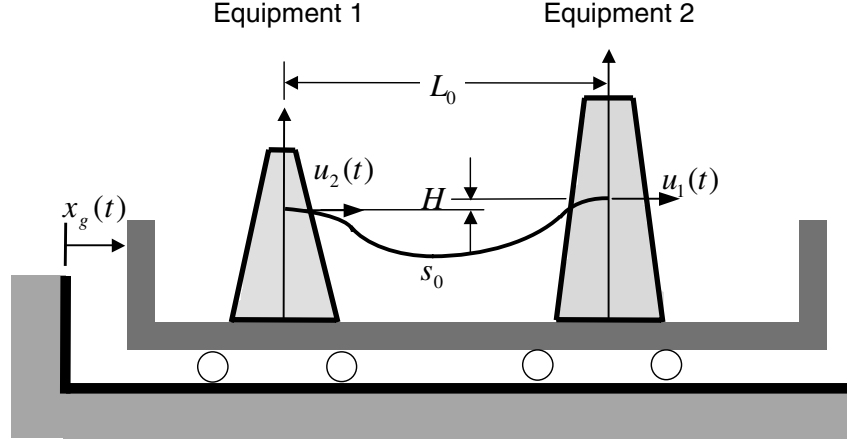


**Figure 6. Model of cable-connected equipment items**

To quantify the effect of interaction, we define the *response ratio*, which was initially introduced in Der Kiureghian [13]. This is the ratio of the maximum displacement response of an equipment item in the connected system to its maximum response in the stand-alone configuration. Thus, denoting the response of the  $i$ -th equipment in its stand-alone configuration as  $u_{i0}(t)$ , the response ratio is

$$R_i = \frac{\max|u_i(t)|}{\max|u_{i0}(t)|}, \quad i = 1, 2 \quad (1)$$

The response ratio provides a dimensionless measure of the interaction effect. A value greater than unity for the response ratio indicates that, on account of the interaction effect in the connected system, the response of the corresponding equipment is amplified relative to its response in the stand-alone configuration; also, a value smaller than unity for the response ratio indicates that the response of the corresponding equipment is deamplified relative to its response in the stand-alone configuration. It is noted that the internal forces in an equipment item, which is modeled as a single-degree-of-freedom system, are directly proportional to the displacement response. Hence, for the assumed model, the above ratios are equally applicable to force responses in the two equipment items. Since equipment items are typically qualified in their stand-alone configurations, the response ratio provides the kind of information that an engineer needs in order to determine whether the equipment item can withstand the amplified seismic demand in the connected system.

While the response ratio provides a good measure of the interaction effect, it involves response quantities that require nonlinear dynamic analysis. For design purposes, it is important to identify simple predictive measures of the interaction effect. A quantity that strongly influences the degree of interaction between the cable-connected equipment items is the maximum distance that the two stand-alone equipment items move away from one another, when subjected to the same ground motion. This quantity is given by

$$\Delta = \max[u_{20}(t) - u_{10}(t)] \quad (2)$$

Obviously, the larger  $\Delta$  is, the larger the interaction effect is likely to be. Another important measure is the amount of slack in the cable. This is measured in terms of the reserve cable length in excess of the chord length, i.e.,  $s_0 - c_0$ . Now suppose one end of the cable is moved horizontally by the amount  $\Delta$ , as shown in Figure 7. In this figure, the solid line indicates the initial position of the cable and the dashed line indicates the displaced position, with  $s$  denoting the current cable length. For  $\Delta$  much smaller than the initial chord length,  $c_0$ , the chord length will increase approximately by the amount  $\Delta L_0 / c_0$ . One can regard this quantity as a measure of the seismic demand on the reserve cable length,  $s_0 - c_0$ , which can be regarded as the corresponding capacity. Obviously, if  $\Delta L_0 / c_0$  is small in relation to  $s_0 - c_0$ , then there will be little interaction between the two equipment items. Conversely, if  $\Delta L_0 / c_0$  is of the same magnitude or greater than  $s_0 - c_0$ , one can expect significant interaction. It follows that the dimensionless parameter can

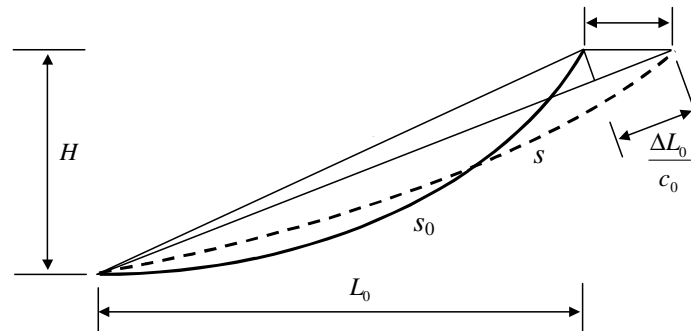


Figure 7. Change in slackness due to relative displacement  $\Delta$

$$\beta = \frac{\Delta L_0 / c_0}{s_0 - c_0} \quad (3)$$

serve as a predictive measure of the interaction effect, and we call it the *interaction parameter*. Other than  $\Delta$ , the parameters in the above expression are readily available from the geometry of the cable. Since  $\Delta$  is defined for the stand-alone equipment items, which by definition are linear and have single degrees of freedom, its determination requires relatively simple analysis. In particular, as shown in Der Kiureghian [13],  $\Delta$  can be conveniently computed by the response spectrum method.

In our earlier study (Der Kiureghian [13]), using a catenary model for the cable, we argued that there will be little interaction between the two equipment items if  $\beta$  is smaller than about 1. On that basis, and to account for a degree of conservatism, we provisionally recommended selecting the cable slackness such that  $\beta$  is no greater than 1. However, the catenary model did not account for the mechanical behavior of the cable, nor for the effect of the cable inertia. Our next study (Der Kiureghian [14], Hong [7]), where we used an elastic rod element for the cable, showed that there could be significant interaction for  $\beta$  values smaller than unity due to the effect of the cable inertia. Based on this study, we recommended selecting the cable slackness such that  $\beta$  is no greater than 1 and designing the equipment items for forces 50% higher than the forces obtained for the stand-alone configuration. In any case, the interaction parameter  $\beta$  remains a good predictor of the interaction effect. In this study, we continue to use this parameter in formulating a predictive model for the response ratio.

## NUMERICAL INVESTIGATION OF INTERACTION EFFECT

In this section, we investigate the effect of interaction by performing nonlinear time-history analyses of example cable-connected equipment systems subjected to selected ground motions. The systems are analyzed by both elastic and elasto-plastic finite-element models of the cable. For the elastic analysis,  $I_{\min}$  is used as the effective moment of inertia of the cable, i.e., the cable is assumed to be in a fully slipped state with zero friction at all times and all cross sections. For the elasto-plastic analysis, the hysteretic model described earlier is used. In both cases, geometric nonlinearities resulting from large displacements and rotations are accounted for. The comparison between the results from the fully-slipped elastic and elasto-plastic models reveals the influence of the variation in the flexural stiffness of the cable (in time and along the cable) in the elasto-plastic model, as well as the dissipation of energy resulting from the slippage of strands. Next, we carry out parametric studies to better understand the relation between the response ratios and the interaction parameter  $\beta$  for different ground motions and conductor cables.

First consider two equipment items connected by the Valerian cable having an initial span  $L_0 = 5\text{m}$  (under static equilibrium conditions), the vertical separation  $H = 0$ , and the initial length  $s_0 = 5.10\text{m}$ . The initial slackness of this cable is  $(s_0 - L_0)/L_0 = 0.02$ . This is a rather taut cable and represents perhaps an extreme case for connected electrical equipment. We select it to highlight the effect of interaction and the highly nonlinear nature of the response. Among the conductor cables used in practice, the Valerian is one of the most flexible having only two layers of strands and the smallest cross-sectional area and moment of inertia (see Table 1). Furthermore, for this cable the ratio of the maximum to minimum moment of inertia is  $I_{\max}/I_{\min} = 22.7$ , which is quite small. The equipment items, modeled as single-degree-of-freedom oscillators, are assumed to have the effective masses  $m_1 = 1000\text{ kg}$  and  $m_2 = 500\text{ kg}$ , natural frequencies  $\omega_1 = 2\pi\text{ rad/s}$  and  $\omega_2 = 10\pi\text{ rad/s}$ , and damping ratios  $\zeta_1 = \zeta_2 = 0.02$ .

We first examine the response of the cable-connected system to the N-S component of the Newhall record of the 1994 Northridge earthquake, which is one of the motions shown in Figure 8. For this record, Figure 9 shows the stand-alone responses,  $u_{10}(t)$  and  $u_{20}(t)$ , of the two equipment items calculated by the HHT algorithm. The calculated maximum stand-alone displacements are  $\max|u_{10}(t)| = 0.3358\text{m}$  and  $\max|u_{20}(t)|$

= 0.0159m, respectively, and the maximum relative separation between the two stand-alone equipment items is  $\Delta = \max|u_{20}(t) - u_{10}(t)| = 0.3163\text{m}$ , yielding the interaction parameter value  $\beta = 3.16$ . The two stand-alone responses are significantly different because of the large difference between the equipment frequencies (1Hz and 5Hz, respectively). These time histories tend to have nearly symmetric peaks relative to the equilibrium positions with nearly zero averages over time.

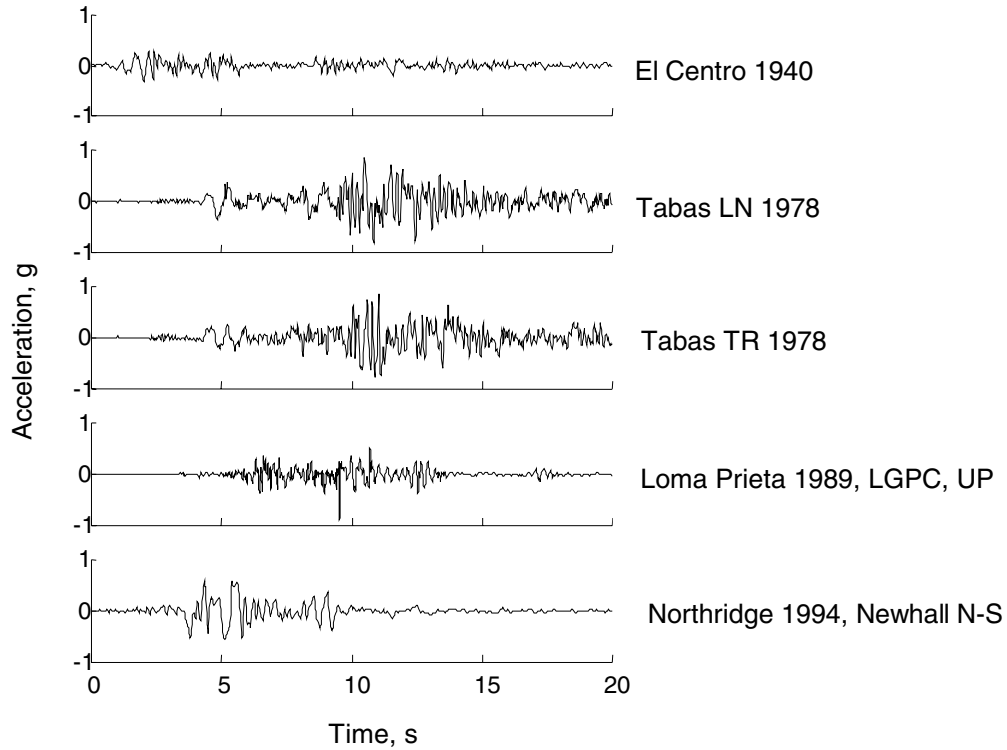


**Figure 8. Selected ground motions**

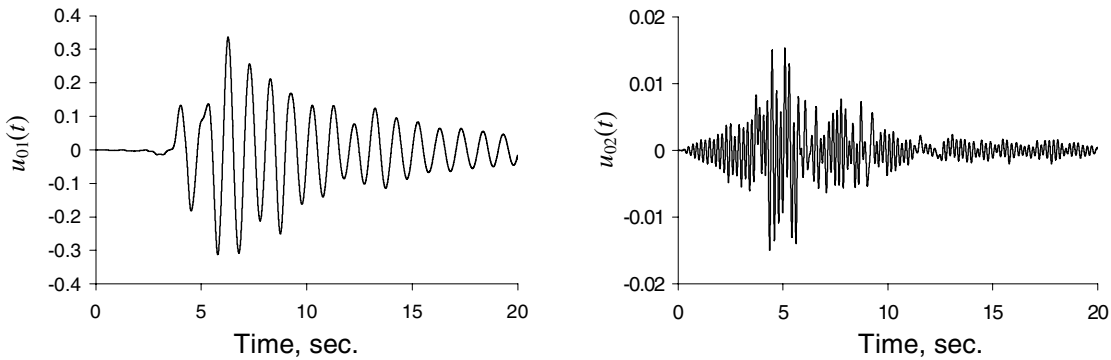


**Figure 9. Stand-alone responses of equipment 1 (left) and equipment 2 (right)**

Figure 10 shows the displacement time histories  $u_1(t)$  and  $u_2(t)$  of the two equipment items in the connected system for the fully-slipped elastic (gray lines) and the elasto-plastic (black lines) finite element models of the Valerian cable. The results of the analyses based on the two models are nearly identical for the lower frequency equipment item (equipment 1), as seen in the left plot in Figure 10. The results for the higher frequency equipment item (right plot in Figure 10) are also similar for the most part, with slightly

smaller peak values for the elasto-plastic case. These results imply that the moment of inertia in the elasto-plastic model remains close to its lower bound at most locations and times. Furthermore, the effect of energy dissipation due to the slippage of strands is insignificant. Recalling that the ratio of moment of inertias  $I_{\max}/I_{\min} = 22.7$  is relatively small for this cable, these findings are not surprising. As we will shortly see, a different result is obtained for heavier conductor cables.

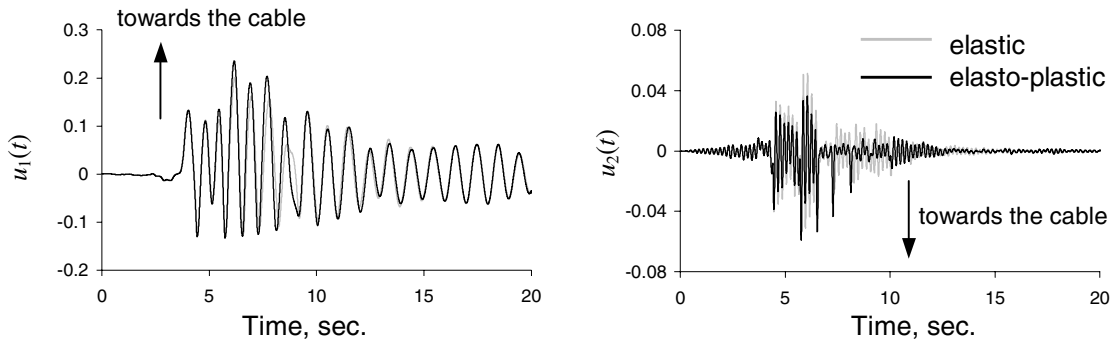


**Figure 10. Displacement responses of equipment 1 (left) and equipment 2 (right) connected by the Valerian cable**

It is noted in Figure 10 that the displacement responses exhibit skewed peaks relative to the equilibrium positions, with non-zero averages over time and larger displacement peaks accruing towards the side that slackens the cable. This is a clear indication of interaction between the two equipment items. Comparing Figures 9 and 10, we observe a decrease in the peak response of equipment 1 (the lower frequency equipment item) in the connected system (Figure 10 left) relative to its stand-alone response (Figure 9 left), and a large increase in the peak response of equipment 2 (the higher frequency equipment item) in the connected system (Figure 10 right) relative to its stand-alone response (Figure 9 right). The response ratios for the two equipment items, based on the elasto-plastic analyses, are  $R_1 = 0.703$  and  $R_2 = 3.71$ , respectively. It is clear that the dynamic interaction adversely affects the higher frequency equipment item. Similar observations were reported in our previous studies (Der Kiureghian [13]-[14], Hong [7]), where we used the catenary formulation or the elastic finite element model of the cable. As described below, it is possible that the lower frequency equipment item also experience amplification of its response due to the cable inertia.

The above analysis is now repeated with the Trillium cable connecting the two equipment items. The Trillium is one of the heaviest of conductor cables used in practice. As shown in Table 1, it has six layers of strands and the ratio of the maximum to minimum moments of inertia is  $I_{\max}/I_{\min} = 160$ . In view of these properties, the plastic energy dissipation of the Trillium cable is expected to be much larger than that of the Valerian cable.

Figure 11 shows the displacement responses  $u_1(t)$  and  $u_2(t)$  of the equipment items in the connected system for the fully-slipped elastic (gray lines) and elasto-plastic (black lines) finite element models of the cable. The two predicted responses now are significantly different. In particular, the peaks in the response time history of the lower frequency equipment item are much smaller for the elasto-plastic predictions, though the extreme peaks are nearly identical. Furthermore, the high frequency content in the response of the higher frequency equipment item has disappeared in the elasto-plastic prediction. These changes can be attributed to the significant energy dissipation that occurs in this cable due to slippage between the strands. Note that the maximum moment of inertia of the Trillium cable is 152 times larger than that of the Valerian cable as shown in Table 1 and, therefore, the yielding moment of the Trillium cable is much larger than that of the Valerian cable. This indicates larger energy dissipation capacity of the Trillium cable

relative to the Valerian cable. The energy dissipation is at least partly responsible for reducing the response peaks and for damping out the higher-frequency components in the response of equipment 2. The response ratios for the two equipment items, based on the elasto-plastic analysis, are  $R_1 = 0.466$  and  $R_2 = 3.65$ . Interestingly, these ratios are not very different from the values observed for the more flexible Valerian cable.

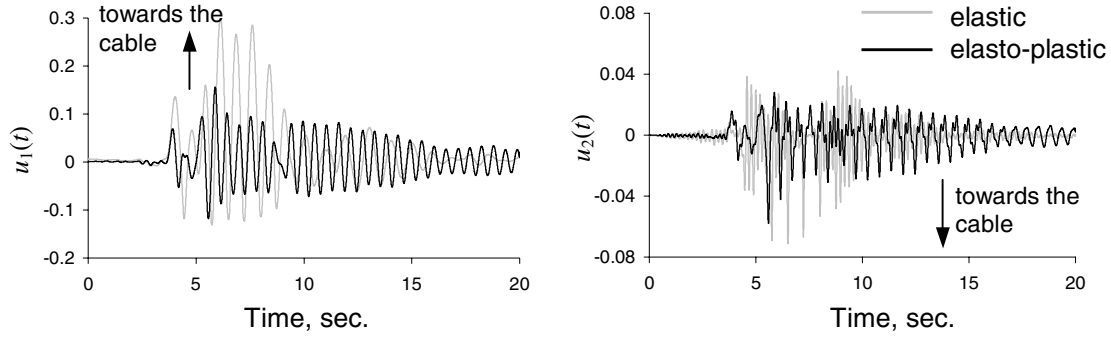
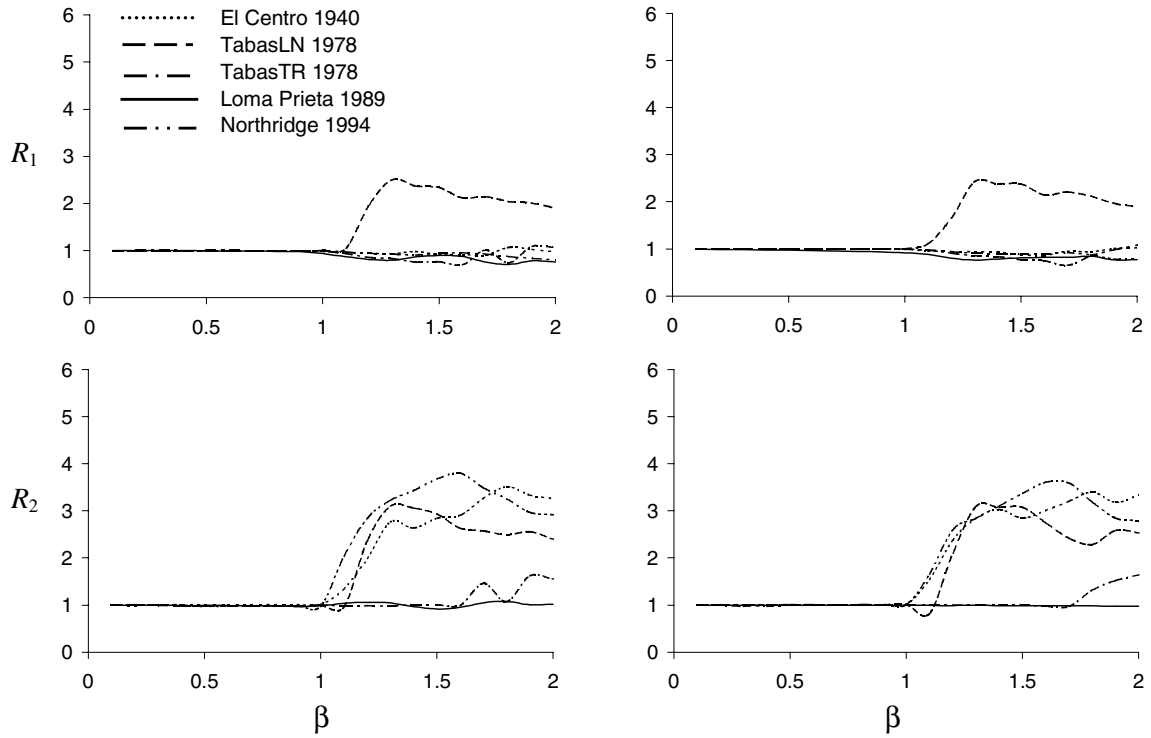


**Figure 11. Displacement responses of equipment 1 (left) and equipment 2 (right) connected by the Trillium cable**

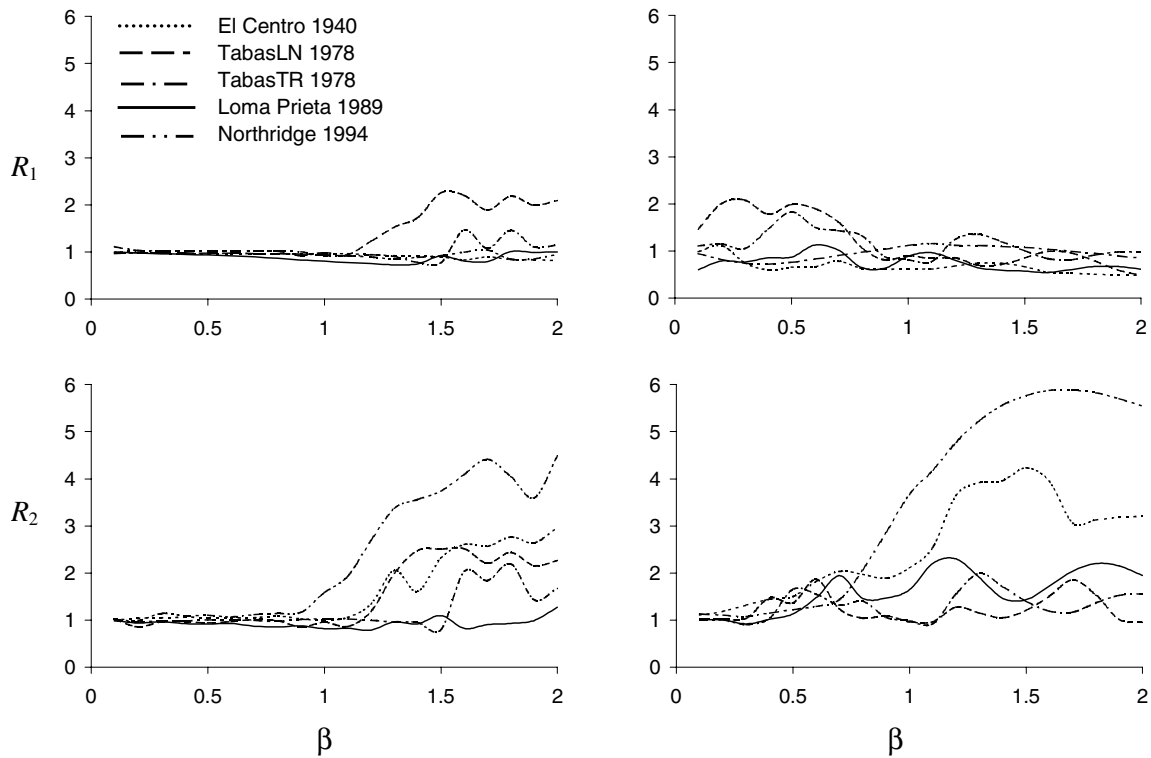
To better understand the effect of interaction between the connected equipment items, we compute and plot the response ratios  $R_1$  and  $R_2$  for the above systems for the five ground motions shown in Figure 8, while varying the interaction parameter  $\beta$  defined in (3). Since the vertical separation between the support points is zero, we have  $c_0 = L_0$  and the interaction parameter for this case simplifies to  $\beta = \Delta/(s_0 - L_0)$ . All system parameters are kept constant, with the exception of the initial cable length  $s_0$ , which is varied to cover the range  $\beta = 0.1$  to  $\beta = 2$  of the interaction parameter.

Figure 12 shows the response ratios  $R_1$  and  $R_2$  of the two equipment items as functions of the interaction parameter  $\beta$  for the system connected by the Valerian cable with the fully-slipped elastic (left) and elasto-plastic (right) models of the cable. The response ratios based on the two models are nearly identical for all values of  $\beta$ . This is due to the high flexibility of the Valerian cable and provides further evidence that the effect of plastic behavior in this cable is practically insignificant. It is observed in this figure that there is virtually no amplification of either equipment response for  $\beta < 1$ . Based on this finding, in our previous study (Hong [7], Der Kiureghian [14]), we recommended a cable length corresponding to  $\beta < 1$  to avoid an adverse interaction effect. This finding remains valid for the Valerian cable.

Figure 13 shows the response ratios  $R_1$  and  $R_2$  of the two equipment items as functions of the interaction parameter  $\beta$  for the system connected by the Trillium cable with the fully-slipped elastic (left) and elasto-plastic (right) models of the cable. The response ratios based on the two models are now entirely different, with the elasto-plastic model showing larger responses for both equipment items in the connected system, including for cases with  $\beta < 1$ . Recall that the elastic model uses the minimum moment of inertia,  $I_{\min}$ , whereas the elasto-plastic model employs a varying moment of inertia with values ranging from  $I_{\min}$  to  $I_{\max}$ . It is clear that the larger effective flexural stiffness associated with the elasto-plastic model induces more interaction between the two equipment items. Another factor contributing to the larger response for small values of  $\beta$  is the mass inertia of the cable itself, which can be quite significant for the Trillium cable when it has a large slack. Resonance-type behavior in the cable is also possibly causing



**Figure 12. Response ratios for equipment items connected by Valerian cable based on fully-slipped elastic (left) and elasto-plastic (right) models of the cable**



**Figure 13. Response ratios for equipment items connected by Trillium cable based on fully-slipped elastic (left) and elasto-plastic (right) models of the cable**

some of the peaks in the  $R_1$  and  $R_2$  plots for this cable. Most importantly, it is clear from this finding that our previous provisional recommendation of determining the cable slackness based on  $\beta = 1$  does not guarantee that there will not be an amplification of the response in the connected system relative to the stand-alone response for either equipment. It appears that for heavy conductor cables similar to the Trillium, an amplification of both equipment responses by as much as a factor of 2 or larger can be expected for  $\beta < 1$ .

It is clear from the above analyses that the interaction effect in cable-connected equipment items subjected to earthquake ground motions is a highly complex phenomenon. This effect depends not only on the equipment and cable characteristics, and this in a rather chaotic fashion, but also on the details of the ground motion. It has been shown (Der Kiureghian [15]) that for a linear connected system, the response ratios are entirely independent of the scaling (intensity) of the ground motion. For a nonlinear system, such as the one under investigation, this generally is not the case. Nevertheless, this observation suggests that the large variability observed in the response ratios in Figures 12 and 13 over the selected ground motions cannot all be attributed to the varying intensities of these motions (Figure 8). It appears that the interaction effect in the cable-connected system is highly sensitive to the details of the ground motion, such as the frequency content, the evolution of intensity in time, the existence of acceleration or velocity pulses, or other such characteristics. In a design situation, it is impossible to correctly predict such detailed characteristics of future earthquakes. Therefore, there is need to develop a method to predict the interaction effect in the cable-connected system, which does not require a detailed specification of the ground motion, but which also accounts for the inevitable variability in the future ground motions. In Hong [4], such a method is developed by use of statistical modeling techniques and simulations generated by the finite element dynamic analysis model described in this paper. Without providing the details, we present here the preliminary form of this predictive model:

$$R = \exp \left[ 0.209 + 0.109 \frac{\omega_{\text{other}}}{\omega_{\text{self}}} + 0.065 \frac{m_{\text{other}}}{m_{\text{self}}} + 0.459 \operatorname{sgn}(\omega_{\text{self}} - \omega_{\text{other}}) \left( 1 + 0.5 \frac{H}{L} \right) \beta + 0.351 \varepsilon \right] \quad (4)$$

In the above expression,  $R$  is the response ratio for an equipment item having an effective mass  $m_{\text{self}}$  and natural frequency  $\omega_{\text{self}}$ , which is cable-connected to another equipment of effective mass  $m_{\text{other}}$  and natural frequency  $\omega_{\text{other}}$ .  $H$  and  $L$  define the geometry of the cable as described in Figure 6, whereas  $\beta$  is the interaction parameter defined in (3). Note that the specification of the ground motion enters this formula through the parameter  $\Delta$ , which is implicit in  $\beta$ . Finally,  $\varepsilon$  is a standard normal random variable (zero mean and unit standard deviation), which accounts for the variability in the response ratio arising from the stochastic nature of the ground motion as well as the chaotic nature of the response of the cable-connected equipment system. For given values of the system and ground motion parameters, this equation can be used to obtain a probability distribution for the response ratio, which can then be used to investigate the safety of the equipment item, or make design provisions. More details about this statistical model will be presented in a future publication.

## SUMMARY AND CONCLUSIONS

The effect of interaction between electrical substation equipment connected by conductor cables is investigated. The conductor cable is made of helically wrapped strands and exhibits complex mechanical behavior due to slippage of the strands under friction. A recently developed model to describe the hysteretic flexural behavior of the conductor cable is briefly outlined. This model is implemented in a finite element formulation that accounts not only for the hysteretic behavior of the cable, but also for its large displacements and rotations under dynamic loading. The finite element model is used to predict the response of example cable-connected systems under selected ground motions. It is found that the equipment response

in the connected system can be much larger (by factors as large as 6) relative to the corresponding response in the stand-alone configuration of the equipment. This finding has a serious implication for electrical substation equipment, which are usually qualified only in their stand-alone configuration neglecting interaction effects.

To reduce the interaction effect, one can increase the cable slackness. However, for heavy cables, this leads to increased influence from the mass inertia of the cable, as a result of which the equipment response may also be adversely affected. A preliminary statistical predictive model is suggested, which attempts to provide a probability distribution for the response amplification, accounting for the stochastic nature of the ground motion and the chaotic nature of the cable response. This formula may be used to predict the adverse interaction effect, so that adequate design provisions can be made.

### ACKNOWLEDGMENT

This paper is based on research supported by the Lifelines Program of the Pacific Earthquake Engineering Research Center funded by the Pacific Gas & Electric Co. and the California Energy Commission. Partial support was also provided by the Earthquake Engineering Research Centers Program of the National Science Foundation under Award No. EEC-9701568. These supports are gratefully acknowledged. The authors wish to thank Eric Fujisaki of PG&E, with whom valuable discussions were held throughout the course of this research.

### REFERENCES

1. Benuska, L. (Editor). "Chapter 8 — Lifelines." *Earthquake Spectra (Supplement)* 1990; 6: 315-338.
2. Hall, J. (Editor). "Chapter 4 — Lifelines." *Earthquake Spectra (Supplement C)* 1995; 11: 188-217.
3. Schiff, A. J. (Editor). "Northridge earthquake: lifeline performance and post-earthquake response." ASCE, New York, NY, 1995.
4. Hong, K.-J. "Dynamic interaction in cable-connected equipment." Dissertation submitted in partial satisfaction of the requirements for the degree of Doctor of Philosophy, University of California, Berkeley, CA, 2003.
5. Hong, K.-J., Der Kiureghian, A. and Sackman, J. L. "Bending behavior of helically wrapped cables." *Journal of Engineering Mechanics*, submitted, 2004.
6. Taylor, R. L. "FEAP Version 7.1 User Manual." Department of Civil and Environmental Engineering, UC Berkeley, CA, 1998.
7. Hong, K.-J., Der Kiureghian, A. and Sackman J. L. "Seismic interaction in cable-connected equipment items." *Journal of Engineering Mechanics*, 2001; 127(11): 1096-1105.
8. Raoof, M. "Free bending tests on large spiral stands." *Proceedings of the Institution of Civil Engineers Part 2*, 1989; 87: 605-626.
9. Cosserat, E., and Cosserat F. "Theory of Deformable Bodies," National Aeronautics and Space Administration, Washington, DC, 1967.
10. Simo, J. C. and Vu-Quoc, L. "On the dynamics of flexible beams under large overall motions — The plane case: Part I." *Journal of Applied Mechanics*, 1986; 53: 849-854.
11. Simo, J. C. and Vu-Quoc, L. "On the dynamics of flexible beams under large overall motions — The plane case: Part II." *Journal of Applied Mechanics*, 1986; 53: 855-863.
12. Hilber, H. M., Hughes, T. J. R., and Taylor, R. L. "Improved numerical dissipation for time integration algorithms in structural dynamics." *Earthquake Engineering and Structural Dynamics*, 1977; 5: 283-292.
13. Der Kiureghian, A., Sackman, J. L., and Hong, K.-J. "Interaction in Interconnected Electrical Substation Equipment Subjected to Earthquake Ground Motions." Report No. PEER 1999/01 University of California, Berkeley, CA, 1999.

14. Der Kiureghian, A., Hong, K-J., and Sackman, J. L. "Further Studies on Seismic Interaction in Inter-connected Electrical Substation Equipment." Report No. PEER 2000/01 University of California, Berkeley, CA, 2000.
15. Der Kiureghian, A., Sackman, J. L., and Hong, K-J. "Seismic interaction in linearly connected electrical substation equipment." *Earthquake Engineering and Structural Dynamics*, 2001, 30: 327-347.